

Hydrosilylation

Chalice-Type Tridentate Silicon Lewis Acids of C₃ Symmetry in a Single Step Starting from Hexadehydrotribenzo[12]annuleneAnna Schwartzen, Jan-Henrik Weddelling, Jana Langosch, Beate Neumann, Hans-Georg Stammer, and Norbert W. Mitzel*^[a]

Abstract: Tridentate Lewis acids with aligned functions were synthesized based on the rigid framework hexadehydrotribenzo[12]annulene. The backbone and its fluorinated analogue were synthesised in one-pot syntheses, with alkyne deprotection and Sonogashira cross coupling reaction being carried out in one step. Hydrosilylation of the annulene with chlorohydrosilanes proceeded highly selectively and afforded rigid poly-Lewis acids with three SiCl₃ or SiCl₂Me substituents perfectly oriented to one side of the molecule in a

single step. The progress of hydrosilylation was investigated by time-correlated NMR spectroscopic studies. The crystal structures show that the framework is symmetrically functionalised and the silyl substituents are aligned in one direction. To increase the acidity of the Lewis acids the chlorosilyl substituents were fluorinated with SbF₃. Further investigation of hydrometallation reactions (M = B, Al, Ga, Sn) did not lead to corresponding structures.

Introduction

Annulenes are macrocyclic through-conjugated hydrocarbon systems.^[1,2] The annulene derivative hexadehydrotribenzo[12]annulene (TBA) exhibits special properties for example, a rigid framework and C₃ symmetry.^[3] The first synthesis of this structure was reported by Eglinton and co-workers in 1966 as reactions between cuprous acetylides and aryl iodides.^[1,4] The trimerisation based on in situ alkyne deprotection and a palladium-copper catalysed reaction of bromophenylacetylene was developed by Linstrumelle and Huynh in 1988.^[5]

Because of the delocalized π -electrons in TBA derivatives, these compounds have been investigated in the field of optoelectronic materials,^[6] aromaticity^[1,7] and formation of transition metal complexes.^[1,8,9] Their rigid framework was basis for the synthesis of multiple-component covalent organic frameworks (COFs),^[10,11] and planar carbon networks.^[1,8,12] The addition of hydrophilic side chains opened the access to liquid-crystalline materials.^[13,14]

In the course of our continued investigation of poly-Lewis acids, we pursued a number of different approaches so far in order to generate rigid and donor-free frameworks that are capable of carrying several Lewis acid functions oriented to the same side of the molecule. Despite the huge body of existing organic compounds, there remains a distinct paucity in frameworks with functionalizable groups only on one side that can serve as donor-free skeletons to construct such poly-Lewis acids. With such directed poly-Lewis acids we aim to define a cavity that binds a Lewis basic substrate in chelating fashion while the defined distances between the binding functions defines chemical selectivity. For bidentate Lewis acids we used for instance dialkynylanthracenes^[15] or diphenyldiethynylsilanes,^[16] diphenyldiethynylsilanes as well as diphenyldiethynylsilanes^[17] to carry two acid functions like B(C₆F₅), AlR₂, GaR₂ and InR₂ (R = Me, Et). Tris-Lewis-acids were realized with trifunctional skeletons including the bowl-shaped tribenzotriquinacene,^[18] tris-(*ortho*-phenyl)-silane,^[19] 1,8,13-substituted triptycenes^[20] or all-*cis*-1,3,5-triethynyl-1,3,5-trisilacyclohexane^[21] carrying the Lewis acid groups. And recently we succeeded in the synthesis of a tetrafunctional Lewis acid with four parallel oriented diphenylboranylethynyl functions attached to the same side of an anthracene dimer. Common to all these examples is the relatively high effort to be spent for their synthesis. It would therefore be highly desirable to find a readily available molecular system that can be addressed by simple reagents to build up such an oriented and spatially defined framework in one step.

In this context TBA's framework seemed well suited for the synthesis of compounds with Lewis-acid functions oriented towards the same direction because of its rigid and donor-free structure. In this contribution we describe that it is possible to use one-pot synthetic strategies to address hexadehydrotribenzo[12]annulenes by hydrometallation of their ethynyl units to

[a] Dr. A. Schwartzen, Dr. J.-H. Weddelling, J. Langosch, B. Neumann, Dr. H.-G. Stammer, Prof. Dr. N. W. Mitzel
Bielefeld University
Universitätsstraße 25, 33615 Bielefeld (Germany)
E-mail: mitzel@uni-bielefeld.de

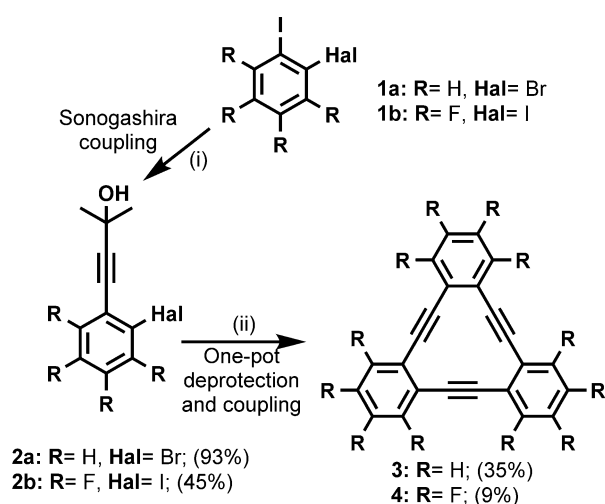
Supporting information and the ORCID identification numbers for the authors of this article can be found under:
<https://doi.org/10.1002/chem.202004088>.

© 2020 The Authors. Chemistry - A European Journal published by Wiley-VCH GmbH. This is an open access article under the terms of the Creative Commons Attribution Non-Commercial NoDerivs License, which permits use and distribution in any medium, provided the original work is properly cited, the use is non-commercial and no modifications or adaptations are made.

achieve exactly this target. In a so far unexpected way, hydrosilylation leads in a highly selective fashion to tridentate Lewis acids with oriented functions, that is, the first step of hydrometallation directs the following two reactions in a regio- and stereoselective way.

Results and Discussion

For the syntheses of tribenzoannulenes (TBA) we used a modified procedure of Huynh et al.^[5] As a simple and economical access to fluorinated benzenes for coupling reactions, we used a modified procedure of Wenk et al. to synthesize iodofluorobenzene **1b**.^[22] Selective Sonogashira coupling reactions^[23,24] starting from the revealing arylhalides (**1a**, **1b**) were used to synthesize the building blocks for trimerisation (**2a**, **2b**; Scheme 1). Because of the same reactivity of the two iodine atoms in the coupling reactions of **1b**, we isolated the doubly alkynylated side product **2c** (6%, Figure 1), which has a very interesting stacking behavior—caused by multiple intermolecular interactions—in the solid state (see Figure S29 in the Supporting Information).



Scheme 1. Synthesis cascade for tribenzo[12]annulenes (TBA) **3** and **4**. Reagents and conditions: i) 1. 2-methyl-3-butyn-2-ol, iPr_2NH , CuI (5 mol.%), **2a**: $PdCl_2(PPh_3)_4$, r.t., 3 d; **2b**: $Pd(PPh_3)_4$, 85 °C, 6 d; 2. aq. workup ii) 1. NaOH, benzene, CuI, benzyltriethylammonium chloride, $PdCl_2(PPh_3)_2$, 3 d, **3**: r.t., **4**: 85 °C; 2. aq. workup.

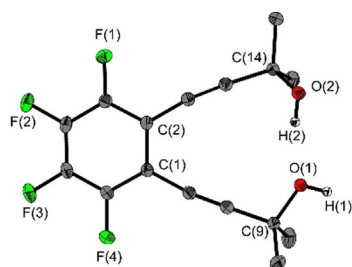


Figure 1. Molecular structure of 1,2-bis(3-methyl-1-butyn-3-ol-1-yl)-3,4,5,6-tetrafluorobenzene (**2c**) in the crystalline state. Hydrogen atoms of methyl groups were omitted for clarity. Thermal ellipsoids are drawn at 50% probability level. H1 and H2 were refined isotropically.

The following one-pot reactions have a great advantage, because the in situ alkyne deprotection of **2a**, **2b** and the cyclo-trimerization reaction can be done without further workup.

The purification by column chromatography was tracked by UV light ($\lambda = 365$ nm) because the compounds fluoresce in yellow. Two new polymorphs of TBA, **3a** and **3b**, were independently found and structurally determined by X-ray diffraction of single crystals (Figure 3). In contrast to the structures determined by Schmidt^[25] and Tagawa,^[26] we found two annulene molecules in each asymmetric unit of the unit cells of polymorphs **3a** and **3b**.

Molecules in **3b** aggregate in dimeric structures with parallel displaced orientation of the annulene molecules, with three independent centroid-centroid distances between the benzene units [4.076(2); 4.620(2); 4.735(2) Å]. Every dimer is corner-connected by an aryl-aryl-interaction between two benzene units [centroid-centroid distance: 3.826(2) Å] leading to polymeric structures along the *c*-axis. The interplanar distance within the dimer of 3.460(2) Å, was defined as the distance between the centroid of the twelve-membered annulene ring to the plane of the neighbouring annulene ring system. The interplanar distances in Figure 2 are displayed as a schematic representation. Molecules of **3a** forms columnar stacks with two different packing motifs **A** and **B** (Figure 2). For motif **A** the edge of one annulene molecule sits right atop the centre of the neighbouring annulene in the crystal lattice, while for motif **B** the annulene molecules overlaps in a side-to-edge motif. The interplanar distances between the twelve-membered annulene centroids and the plane of the neighbouring layers within the columns are slightly different [**A**: 3.315(1) Å; **B**: 3.371(1) Å]. Additionally, multiple aryl-aryl and aryl-acetylene interactions can be found (Table 1). **3a** is the first columnar structure found for 5,6,11,12,17,18-hexadehydrotribenzo[a.e.i.]cyclododecene **3** known so far.

We also tested the alternative step-by-step protocols for TBA **3**. In these procedures, starting from 1-bromo-2-iodobenzene^[27] or 2-iodoaniline,^[28] the annulene derivatives are built up by alternating coupling and deprotection reactions. These syntheses are considerably more complex and achieve no higher yields than the one-pot synthesis for TBA **3** described above (one-pot: 35%, step-by-step: 34%^[29]).

Fluorinated TBA **4** was prepared under analogous conditions with the usual low yields (9%, lit. 8%^[30]) for cyclisation reactions of tribenzoannulenes.^[31] The biggest problem for the cyclisation reactions is the formation of higher homologues like octadehydrotetrabenzo[16]annulenes (QBAs, Figure 3) and recently has been investigated in detail by Baxter et al.^[32] Many conditions were tested to investigate their effect on the formation of side-products, but the relationships still remain unresolved. We also observed the formation of these side-products during our one-pot syntheses for tribenzo[12]annulenes **3** and **4** via NMR-spectroscopy. Unexpectedly, we obtained very small amounts of single-crystalline material of 1,2,3,4,7,8,9,10,13,14,15,16,19,20,21,22-hexadecafluoro-5,6,11,12,17,18,23,24-octadehydrotetrabenzo[a.e.i.m.]cyclohexadecene (QBA **4a**), which has not been described so far.

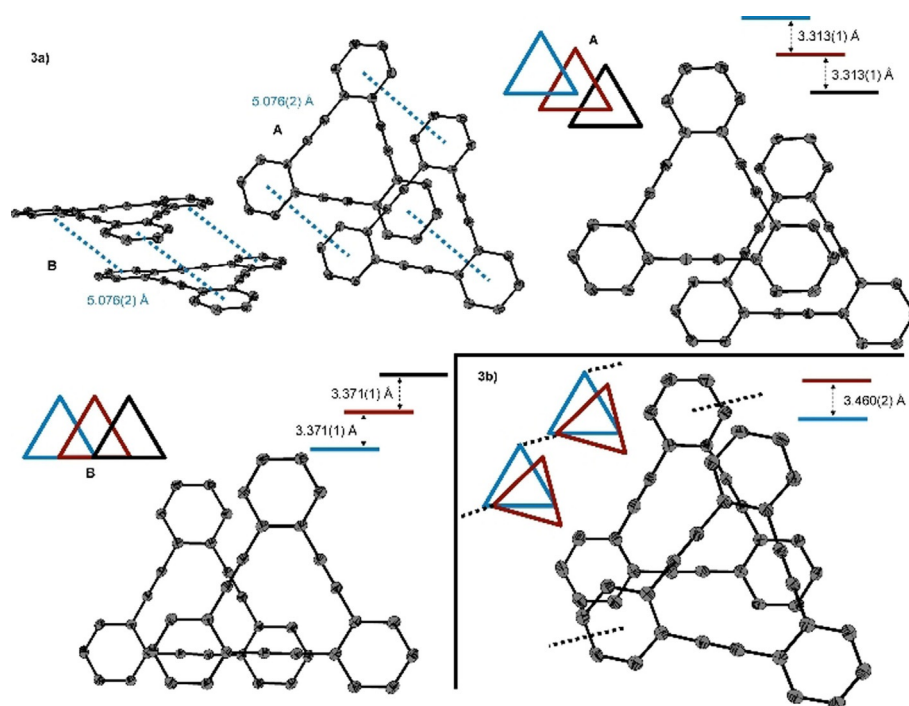


Figure 2. Molecular structures and aggregation of **3a/b** in the crystalline state. Displacement ellipsoids are drawn at 50% probability level. Hydrogen atoms are omitted for clarity. The interplanar distances are displayed as a schematic representation. Both solid-state structures contain two annulene molecules in the asymmetric unit. **3b**: parallel displaced dimer, **3a**: columnar stacks, with packing motifs **A**, **B**. Symmetry operation for generating equivalent positions: **3a**: $+x, +y, -1+z$; **3b**: $1+x, +y, +z$.

Compound	3b	3a	
packing motif	–	A	B
Interplanar distance [Å]	3.460(2)	3.315(1)	3.371(1)
$d_{\text{centr-centr}}$ [Å]	4.076(2)	5.072(1)	4.651(1)
	4.620(2)	5.076(1)	5.076(1)
	4.735(2)	5.307(1)	
	3.826(2)		
$d_{\text{centr-C}\equiv\text{C}}$ [Å]	3.346(2)	3.729(1)	3.373(1)
	3.369(1)	3.964(1)	3.444(1)
	4.048(1)	3.987(1)	
		3.736(1)	
		3.785(1)	
$d_{\text{C-C}}$ [Å]	3.190(5)	3.254(3)	
	(C3–C30)	(C35–C40)	

The columnar arrangement of QBA **4a** is not common for such tetrabenzo[16]annulenes. Usually they prefer to aggregate in chains with only two intermolecular benzene-benzene contacts between the neighboring molecules in the crystal lattice.^[33] The molecule resides on a two-fold axis of the space group $C2/c$, so it shows a perfect columnar arrangement with a distance between the layers and the benzene units corresponding to the length of the b -axis of 3.710(1) Å. The backbone is clearly non-planar, with the tetrafluorobenzene groups being alternately directed up and down, the mean plane

angles of the benzene rings to the a - c plane of the unit cell are 24.3(1)° resp. 24.0(1)°; they form an angle of 33.8(1)° with each other. This strong distortion is not surprising, because the angles of the four *ortho*-positioned acetylene groups add up to 240° instead of 360°, which is required for a relaxed ring system. All bond angles of the ring system change so that they reduce this steric pressure (see Table S2). This arrangement is not favored by aromatic ring systems because of electrostatic repulsion of their quadrupoles. Our group recently found the eclipsed orientation of perhalogenated flexibly-linked aryl groups to be stabilized by London dispersion interactions ($C_6H_5 < C_6F_5 < C_6Cl_6$).^[34]

Overall we have established protocols for the synthesis of TBAs **3** and **4** in a few steps and acceptable yields. In the following we describe hydrometallation reactions using these TBAs.

Hydrosilylation reactions

Tribenzo[12]annulene **3** was converted into triply silylated compounds with $SiCl_2Me$ and $SiCl_3$ groups in hydrosilylation reactions of TBA **3** with $HSiCl_2Me$ and $HSiCl_3$, respectively (Scheme 2). The reactions were conducted in the corresponding silane as solvent. The conversion of the TBA **3** can also be monitored using UV light. The initial yellow fluorescence of the solution turns into deep blue after completion of the hydrosilylation.

The hydrosilylation reaction of TBA **3** with trichlorosilane does not proceed quantitatively. It remains incomplete even

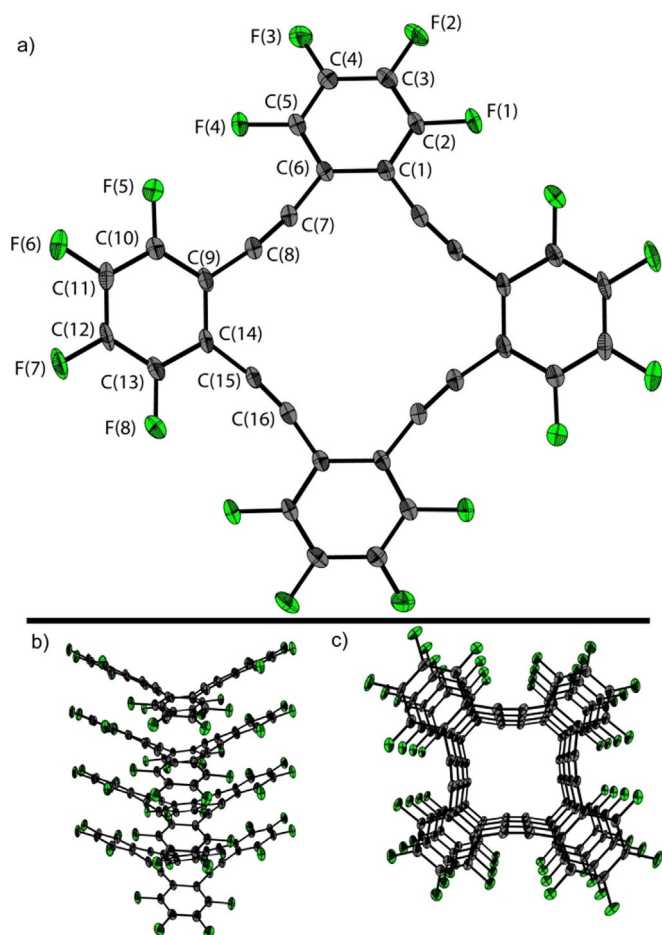
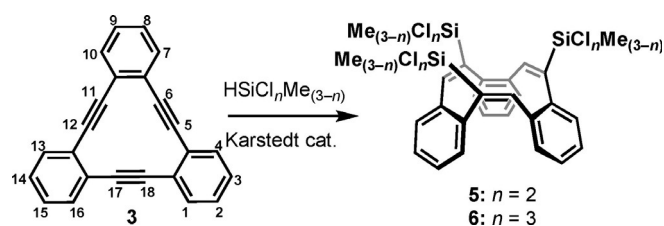


Figure 3. Molecular structure and aggregation of 1,2,3,4,7,8,9,10,13,14,15,16,19,20,21,22-hexadecafluoro-5,6,11,12,17,18,23,24-octadehydrotetrabenzo[a.e.i.m]-cyclohexadecene (QBA 4a) in the crystalline state. Displacement ellipsoids are drawn at 50% probability level. a) Molecular structure and labeling, b) side on view on columnar structure, c) top view on columns. Symmetry operation for generating second part of molecule $(1+x, +y, 3/2-z)$ and equivalent positions: $+x, -1+y, +z$.



Scheme 2. Hydrosilylation reaction of annulene **3** with HSiCl_2Me and HSiCl_3 . Reagents and conditions: i) $\text{HSiCl}_n\text{Me}_{3-n}$, Karstedt's catalyst (2.2–2.4% Pt in xylene), r.t., 4 h (**5**), 7 d (**6**), 90–97%.

after one week of reaction time, although trichlorosilane was expected to be more reactive than methylchlorosilane. The SiCl_2Me -substituted product **5** could be purified by sublimation, while there remain some impurities in the case of **6**. Annulene **3** was also reacted with dimethylchlorosilane, HSiClMe_2 , but this reaction proceeded with low conversion rates and in an unselective manner. An increase in catalyst or silane concentration did not improve the yields.

Chlorosilanes **5** and **6** are of course mixtures of their two enantiomers. These cannot be distinguished by NMR spectroscopy and mass spectrometry. However, surprising is the fact that only hydrosilylation products of C_3 symmetry are obtained, that is, the hydrosilylation takes place for all three CC triple bonds from the same side of the molecule and with the same regioselectivity.

This demonstrates impressively that the first step of hydrosilylation on the annulene framework determines the regio- and stereoselectivity of the two consecutive reactions.

The ^1H NMR spectrum of annulene **3** shows two multiplets at 7.35 and 7.18 ppm with an integral ratio of 1:1 (Figure 4), due to the D_{3h} symmetry of the molecule. The ^1H NMR spectra of the chlorosilanes **5** and **6** (Scheme 2) show that the protons at the benzene rings generate four signals, two doublets and two triplets. Downfield-shifted singlets belong to the vinyl protons. In addition, compound **5** shows a highfield-shifted singlet for the methyl protons of the silyl functions.

The molecular ion peaks in the EI mass spectra of both chlorosilanes **5** and **6** are of low intensity and the fragmentation patterns indicate the elimination of the corresponding silyl groups. Selected ^1H and $^{29}\text{Si}\{^1\text{H}\}$ NMR chemical shifts of the chlorosilanes **5** and **6** in CDCl_3 at ambient temperature are listed in Table 2. These resonance patterns are proof for the C_3 symmetry of the triple hydrosilylation products, lower symmetry would require more signals to be observed. Elemental analyses of compounds **5** and **6** proved their identity, although

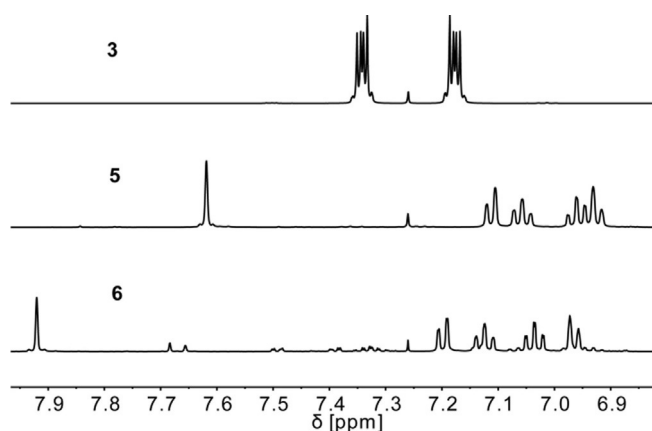


Figure 4. Comparison of the ^1H NMR spectra of tribenzoannulene **3** and its hydrosilylation products with HSiCl_2Me (\rightarrow **5**) and HSiCl_3 (\rightarrow **6**) in CDCl_3 .

Table 2. Selected ^1H and $^{29}\text{Si}\{^1\text{H}\}$ NMR chemical shifts (ppm) of compounds **5** and **6** in CDCl_3 solution. For numbering, see Scheme S1 in the Supporting Information.^[35]

Compound	5 (SiCl_2Me)	6 (SiCl_3)
Ar-CH=	7.62 (s)	7.91 (s)
H4/H10/H16	7.11 (dd)	7.11 (dd)
H3/H9/H15	7.06 (dt)	7.12 (dt)
H2/H8/H14	6.96 (dt)	7.03 (dt)
H1/H7/H13	6.92 (dd)	6.96 (dd)
$\text{SiCl}_n\text{Me}_{3-n}$	14.6	−6.1

carbon values were slightly too low, probably due to silicon carbide formation.

The SiCl_2Me substituted TBA **5** crystallises as racemic twin in the orthorhombic space group $P2_12_12_1$ with four molecules per unit cell (Figure 5). The proof of symmetrical hydrosilylation by NMR spectroscopy is fully confirmed by the molecular structure in the crystal. It shows that the three benzene rings are bent towards one side of the molecule to form a chalice-type structure. The cavity formed by these benzene groups can be described by their distances of the centroids [4.550(1)–4.926(1) Å]. Consequently, the three silyl functions on the other side of the molecule are also aligned into one direction. The distances between the silicon atoms, which are potential acceptor functions, are in a range between 5.600(1) and 5.853(1) Å. Furthermore, the double bond surroundings are not planar because the chlorosilyl functions are bent outwards. Thus, the torsion angles defining the silicon positions are significantly less than 180° [C(23)–C(24)–C(1)–Si(1) $169.4(2)^\circ$, C(7)–C(8)–C(9)–Si(2) $170.2(2)^\circ$, C(15)–C(16)–C(17)–Si(3) $166.8(2)^\circ$]. All other bond lengths and angles are in the range of expected values and deserve no detailed discussion.

The progress of hydrosilylation was monitored time-dependently by NMR spectroscopy. The lower spectrum in Figure 6 is that of the starting material before addition of the catalyst and the upper one the product spectrum. Five minutes after catalyst addition, the NMR spectrum still shows mainly starting

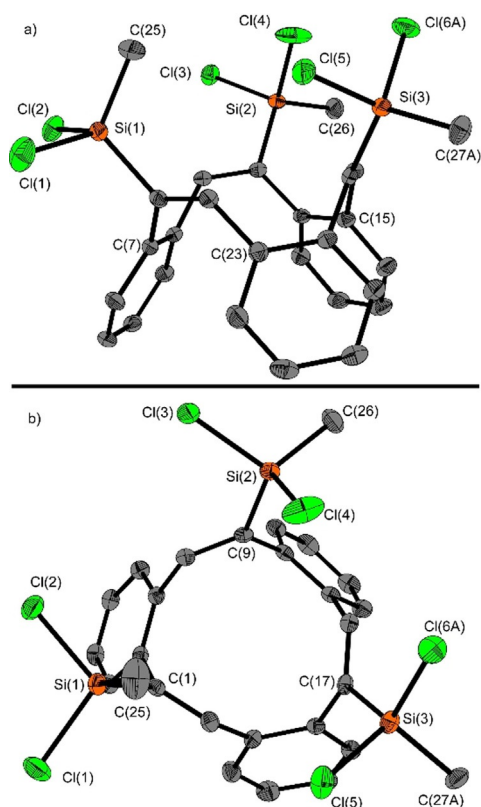


Figure 5. Molecular structure of compound **5** in the crystalline state. Displacement ellipsoids are drawn at the 50% probability level. Disorder of C(27) and Cl(6) over two sites (56:44). Minor occupied disordered atoms and hydrogen atoms are omitted for clarity. a) side on view; b) top view.

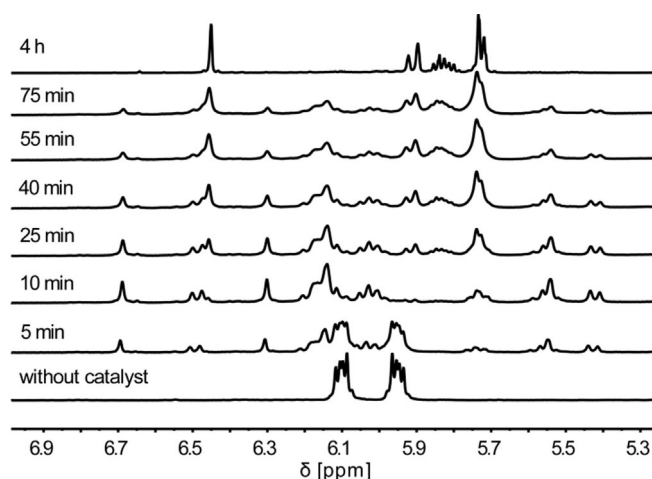


Figure 6. ^1H NMR spectra of the hydrosilylation of **3** with HSiCl_2Me at different reaction times.

material, but also signals of lower intensity for new compounds.

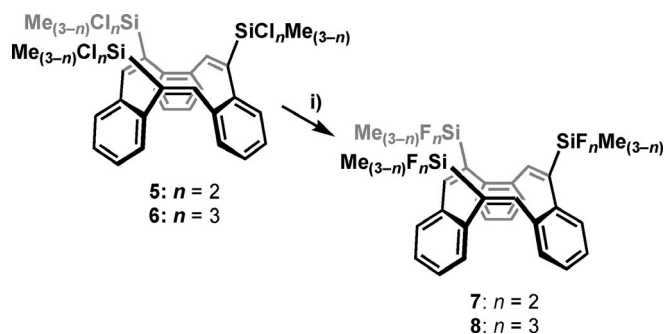
In the spectrum range for vinyl protons, several new resonances are observed. This suggests that singly and doubly hydrosilylated products have already been formed. After 25 minutes, these product signals are clearly visible and subsequently decrease in intensity, while those signals belonging to the final product continuously increase in intensity. Complete hydrosilylation of annulene **3** is achieved after approximately four hours, visible in the spectra by a significant simplification of the spectrum (Figure 6). These results suggest that the first two hydrosilylation steps are relatively fast, while the last slower step of hydrosilylation determines the overall reaction speed.

We also tried to convert fluorinated tribenzo[12]annulene **4** in hydrosilylation reactions. The yellow solution of TBA **4** in HSiCl_2Me turned orange, 30 minutes after adding Karstedt's catalyst, but the ^{19}F NMR spectrum after workup showed the formation of many different products. Increase of the catalyst and application of higher temperatures as well as a change of solvents did not lead to a useful symmetric conversion.

Fluorination reactions

The Lewis acidity of the chlorosilyl substituted compounds can be increased by substitution with fluorine atoms. In order to achieve this, Lewis acids **5** and **6** were reacted with antimony trifluoride (SbF_3) in *n*-pentane (Scheme 3). The reaction solutions were filtered and residues of SbCl_3 were separated by sublimation. We attempted to determine several crystal structures of fluorosilanes containing different amounts of SbCl_3 . Due to severe disorder in the crystal and poor *R*-values, we do not report more details of these structures, but note that the antimony atoms lie in chalice of the backbone, as reported for other chalice-shaped triaryl complexes of SbCl_3 .^[19]

The ^1H NMR spectra of compounds **7** and **8** show similar signal patterns as compounds **5** and **6**, but all signals for the protons at the benzene rings are slightly low-field shifted. In



Scheme 3. Syntheses of **7** and **8** by fluorination of **5** and **6** with SbF_3 (only one of the enantiomers is shown). Reagents and conditions: i) SbF_3 , *n*-pentane, r.t., 24 h, 94–95%.

addition, the resonances of these protons are closer to each other compared to the resonances of the chlorosilanes **5** and **6**. The vinylic proton signals are high-field shifted (Table 2) compared with the those of the chlorinated analogues. In the $^{13}\text{C}\{^1\text{H}\}$ NMR spectrum of compound **7**, all carbon atoms in the vicinity of the fluorinated silyl function show a triplet splitting due to the coupling to the fluorine atoms of the SiMeF_2 groups. Analogously, the $^{13}\text{C}\{^1\text{H}\}$ NMR spectrum of compound **8** shows corresponding quartet splitting by the SiF_3 groups. The ^{29}Si resonances of the silicon atoms of compounds **7** and **8** are strongly low-field shifted due to the substitution of chlorine by fluorine atoms (Table 3).

Compound	7 (SiF_2Me)	8 (SiF_3)
Ar-CH=	7.47 (s)	7.71 (s)
H4/H10/H16	7.15 (m)	7.23 (d)
H3/H9/H15	7.11 (m)	
H2/H8/H14	7.06 (dd)	7.19–7.15 (m)
H1/H7/H13	7.01 (m)	7.07 (d)
$\text{SiCl}_n\text{Me}_{3-n}$	−15.3 (t)	−78.5 (q)

In one experiment, we conducted a hydrosilylation and subsequent fluorination, without further purification of the chlorosilane species. Derivate **9**, which has its origin in an intermediate of an incomplete hydrosilylation, was crystallized. The molecular structure was determined by X-ray diffraction and is depicted in Figure 7. The derivate **9** crystallises in the triclinic space group $P\bar{1}$ with two molecules per unit cell. The single crystals were obtained by slow evaporation of saturated *n*-pentane solution. In the resulting molecular structure the distance between the two silicon atoms is 5.342(1) Å. Compared to the Si-Si distances in the crystal structure of compound **5** [5.600(1)–5.853(1) Å], the distance in the doubly hydrosilylated annulene derivative is significantly shorter. The reason for this is the rigid triple bond, which prevents the silyl functions to be turned outwards any further. Additionally, the triple bond deviates from linearity in the crystal structure. The angle C(16)–C(17)–C(18) is 171.8(1)° and the angle C(17)–C(18)–C(19) is 175.0(1)°.

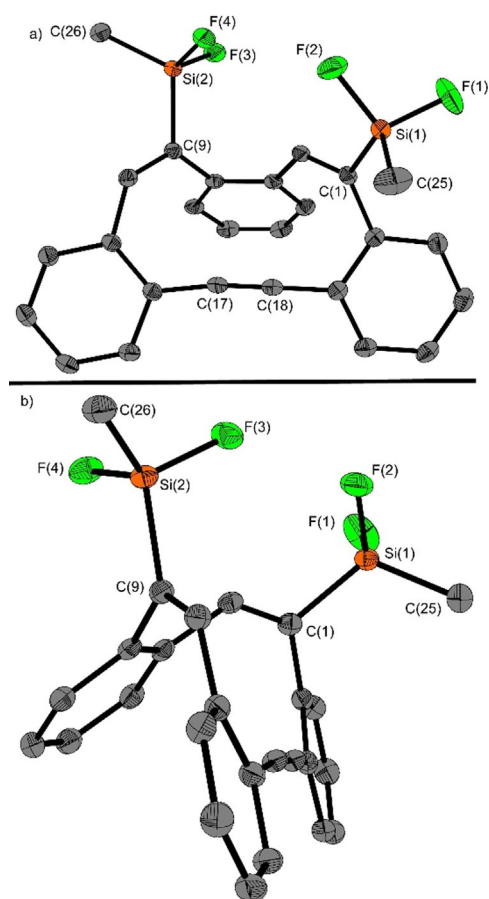


Figure 7. Molecular structure of the annulene derivative **9** with two SiF_2Me groups in the crystalline state. Displacement ellipsoids are drawn at the 50% probability level. Hydrogen atoms are omitted for clarity.

The benzene rings at the ends of the triple bond are slightly twisted against each other with an angle between the best two ring planes of 6.4(1)°.

This structure helps to rationalize the selectivity of the above described hydrosilylation reactions. Hydrosilylation of the first triple bond of annulene **3** results in a double bond and a bending of the two adjacent benzene rings to the same side which induces one side of the product molecule to be less accessible than the other. The second hydrosilylation takes place from the better accessible side and at the most reactive remaining triple bond, and probably sterically steered into the most distant position between the two silyl groups. This leads to a situation similar to that of the structure of **9**. The remaining rigid triple bond is already bent in the way the double bond formed in the next hydrosilylation step is, resulting in a clear preference of the side from which the third hydrosilylation attack will happen.

The initial intention of this work was to find a new access to triple Lewis acids with a directed alignment of the acceptor functions. Therefore, the Gutmann–Beckett method was used to evaluate the Lewis acid quality of the new tridentate silicon Lewis acids **5–8**.^[36,37] For this purpose, compounds **5** and **7** were dissolved in deuterated chloroform and triethylphosphine oxide was added. The ^{31}P shift was then measured using NMR

Table 4. $^{31}\text{P}\{^1\text{H}\}$ NMR chemical shifts [ppm] of compounds **5** and **7** with OPEt_3 in CDCl_3 solution.

Compound	$\text{SiX}_n\text{Me}_{(3-n)}$	$\delta^{31\text{P}}$	$\Delta^{31\text{P}}$	AN ^[a]
OPEt_3	–	52.3	–	–
5	SiCl_2Me	54.8	2.5	31
7	SiF_2Me	66.7	14.4	57

[a] $\text{AN} = 2.21 \times (\delta^{31\text{P}}_{\text{LA-TEPO}} - 41)$, Gutmann–Beckett method.^[37]

spectroscopy, giving a relative value for Lewis acidity (Table 4). The other two silane compounds were not measured because of too small amounts of product.

The measured values show that chlorosilane **5** causes a slight shift of 2.5 ppm and thus represents a relatively weak Lewis acid. The fluorinated compound, on the other hand, leads to a ^{31}P shift of 14.4 ppm, that is, six times greater than that of compound **5**, indicating this fluorosilane compound to be a much stronger Lewis acid.

Comparison with other Lewis acidities of silicon Lewis acids is difficult because there are only a few measured values reported in the literature.^[38] Instead, the boranes are a well-studied class of compounds and serve to classify the measured values.^[39] Chlorosilane **5** with an acceptor number of 31 is comparable to $\text{B}(\text{OCH}_2\text{CH}_2\text{Cl})_3$ (neat, $\text{AN} = 31$)^[39] and fluorosilane **7** to $\text{B}(\text{C}_6\text{H}_5)_3$ (C_6D_6 , $\text{AN} = 55$).^[40] Compared to the strong Lewis acids BF_3 (CDCl_3 , $\text{AN} = 84$)^[41] and $\text{B}(\text{C}_6\text{F}_5)_3$ (CD_2Cl_2 , $\text{AN} = 80$),^[42] chlorosilane **5** is a weak Lewis acid and fluorosilane **7** ranges in the midfield.

We have tried to convert Lewis acid **7** into acid-base adducts using a neutral guest molecule with three Lewis basic functions. Upon addition of an equimolar amount of 1,3,5-trimethyl-1,3,5-triazacyclohexane (TMTAC) to a solution of the fluorosilane **7** in CDCl_3 solution, a fine colourless solid precipitated. This solid compound was insoluble in any common solvents and was therefore not further investigated and characterised.

Hydrometallation reactions

We attempted to use annulene derivatives **3** and **4** also in other hydrometallation reactions, with hydrometallation reagents of the elements of main group III ($M = \text{B}, \text{Al}, \text{Ga}$) and IV ($M = \text{Si}, \text{Sn}$). We tried different methods and varied parameters like temperature, reaction time or the solvent. In addition, some of the reactions were conducted in the presence of a catalyst. The reagents and parameters are shown in Table S1 in the Supporting Information. Despite these many attempts and for none of these cases, we were able to isolate the predicted products. In most of the reactions we could not see a conversion, monitored by the corresponding resonances in ^1H or $^{19}\text{F}\{^1\text{H}\}$ NMR spectroscopy. For such cases where a conversion could be observed, the generated products could not be identified or decomposed after a short time. We suspected an incomplete and/or unsymmetrical substitution, because of the many different resonance patterns we observed in the NMR spectra. The fact that only symmetrical products were obtained for hydrosilylation with HSiCl_3 and HSiCl_2Me is not fully under-

stood. The analogous reaction with HSiClMe_2 under the same conditions did not lead to the predicted products. On the one hand the acetylene bond might not be polar enough for some of the reagents, on the other hand hydrometallation reagents, which are highly reactive, lead to unsymmetrical products.

Conclusion

5,6,11,12,17,18-Hexadehydrotribenzo[a.e.]cyclododecene (**3**) as well as its fluorinated analogue (**4**) have been synthesized in one-pot synthesis protocols and were characterized by X-ray diffraction. First columnar structures for tribenzo[12]annulene **3** and fluorinated side product 1,2,3,4,7,8,9,10,13,14,15,16,19,20,21,22-hexadecafluoro-5,6,11,12,17,18,23,24-octadehydrotetrazobenzocyclohexadecene **4a** were found. By hydrosilylation reactions with HSiCl_2Me (\rightarrow **5**) and HSiCl_3 (\rightarrow **6**) the planar tribenzo[12]annulene (**3**) was converted into tridentate silicon Lewis acids. Molecules **5** and **6** are of molecular C_3 symmetry, are chiral and are obtained as racemates. In these reactions the first step of the hydrosilylation determines in high regio- and stereoselectivity the following two steps. The molecular structure of compound **5** in the solid state shows that the benzene rings are bent towards one side of the molecule thus forming a chalice-type structure. The silyl groups are oriented to the opposite side of the molecule. The described reaction transforms a planar hydrocarbon system into a trifunctional system with oriented functions in a single step. The process of the hydrosilylation reaction was monitored by NMR spectroscopy. It unravelled the first two hydrosilylation steps to proceed relatively quickly, while the third and last step of hydrosilylation is slower. Chlorosilanes **5** and **6** were converted into fluorosilanes **7** and **8** with SbF_3 to increase their Lewis acidities. This increase was confirmed by the Gutmann-Beckett method of relative acidity measurement.

Hydroboration, hydrogallation, hydroalumination and hydrostannylation reactions with the tribenzo[12]annulenes **3** and **4** were also attempted. However, none of those reactions led to identifiable or isolable products. In most cases no conversion was observed via ^1H or $^{19}\text{F}\{^1\text{H}\}$ NMR spectroscopy. For those where a reaction took place, the products decomposed over time or the substitution of the acetylene bonds proceeded unsymmetrically or incompletely.

However, due to the high potential of the possibility to obtain chalice-like compounds in a single step of synthesis we will test parameters for other hydrometallation reagents in the future in order to explore if the phenomenon of regio- and stereoselective substitution can be extended to more examples than reported herein.

Experimental Section

Deposition numbers 2013924 (**1b**), 2013925 (**2c**), 2013926 (**3a**), 2013927 (**3b**), 2013928 (**4a**), 2013929 (**5**), and 2013930 (**9**) contain(s) the supplementary crystallographic data for this paper. These data are provided free of charge by the joint Cambridge

Crystallographic Data Centre and Fachinformationszentrum Karlsruhe Access Structures service.

Acknowledgements

We thank Klaus-Peter Mester and Marco Wißbrock for recording NMR spectra and Barbara Teichner for elemental analyses. This work was funded by Deutsche Forschungsgemeinschaft (DFG, German Research Foundation, grant MI477/39-1, project number 424957011). Open access funding enabled and organized by Projekt DEAL.

Conflict of interest

The authors declare no conflict of interest.

Keywords: annulenes · chalice structure · hydrosilylation · solid-state structures · tridentate Lewis acids

- [1] E. L. Spitler, C. A. J. li, M. M. Haley, *Chem. Rev.* **2006**, *106*, 5344–5386.
- [2] H. A. Staab, F. Graf, K. Doerner, A. Nissen, *Chem. Ber.* **1971**, *104*, 1159–1169.
- [3] a) M. Dudič, I. Císařová, J. Michl, *J. Org. Chem.* **2012**, *77*, 68–74; b) I. Hisaki, H. Senga, Y. Sakamoto, S. Tsuzuki, N. Tohnai, M. Miyata, *Chem. Eur. J.* **2009**, *15*, 13336–13340; c) I. Hisaki, H. Senga, H. Shigemitsu, N. Tohnai, M. Miyata, *Chem. Eur. J.* **2011**, *17*, 14348–14353.
- [4] I. D. Campbell, G. Eglinton, W. Henderson, R. A. Raphael, *Chem. Commun. (London)* **1966**, 87–89.
- [5] C. Huynh, G. Linstrumelle, *Tetrahedron* **1988**, *44*, 6337–6344.
- [6] a) J. J. Pak, T. J. R. Weakley, M. M. Haley, *J. Am. Chem. Soc.* **1999**, *121*, 8182–8192; b) M. Sonoda, Y. Sakai, T. Yoshimura, Y. Tobe, K. Kamada, *Chem. Lett.* **2004**, *33*, 972–973.
- [7] J. Jusélius, D. Sundholm, *Phys. Chem. Chem. Phys.* **2001**, *3*, 2433–2437.
- [8] U. H. F. Bunz, Y. Rubin, Y. Tobe, *Chem. Soc. Rev.* **1999**, *28*, 107–119.
- [9] a) J. D. Ferrara, C. Tessier-Youngs, W. J. Youngs, *J. Am. Chem. Soc.* **1985**, *107*, 6719–6721; b) J. D. Ferrara, A. Djebli, C. Tessier-Youngs, W. J. Youngs, *J. Am. Chem. Soc.* **1988**, *110*, 647–649.
- [10] J. W. Crowe, L. A. Baldwin, P. L. McGrier, *J. Am. Chem. Soc.* **2016**, *138*, 10120–10123.
- [11] J. W. Crowe, *Dissertation: Design and Synthesis of Dehydrobenzoannulene Based Covalent Organic Frameworks*, The Ohio State University, **2018**.
- [12] J. A. Marsden, M. M. Haley, *J. Org. Chem.* **2005**, *70*, 10213–20226.
- [13] K. Tahara, K. Kaneko, K. Katayama, S. Itano, C. H. Nguyen, D. D. D. Amorim, S. De Feyter, Y. Tobe, *Langmuir* **2015**, *31*, 7032–7040.
- [14] S. H. Seo, T. V. Jones, H. Seyler, J. O. Peters, T. H. Kim, J. Y. Chang, G. N. Tew, *J. Am. Chem. Soc.* **2006**, *128*, 9264–9265.
- [15] a) J. Chmiel, B. Neumann, H.-G. Stammer, N. W. Mitzel, *Chem. Eur. J.* **2010**, *16*, 11906–11914; b) J.-H. Lamm, P. Niermeier, A. Mix, J. Chmiel, B. Neumann, H.-G. Stammer, N. W. Mitzel, *Angew. Chem. Int. Ed.* **2014**, *53*, 7938–7942; *Angew. Chem.* **2014**, *126*, 8072–8076.
- [16] J. Horstmann, M. Hyseni, A. Mix, B. Neumann, H.-G. Stammer, N. W. Mitzel, *Angew. Chem. Int. Ed.* **2017**, *56*, 6107–6111; *Angew. Chem.* **2017**, *129*, 6203–6207.
- [17] J. Horstmann, M. Niemann, K.-N. Berthold, A. Mix, B. Neumann, H.-G. Stammer, N. W. Mitzel, *Dalton Trans.* **2017**, *46*, 1898–1913.
- [18] J. Tomaschautzky, B. Neumann, H.-G. Stammer, N. W. Mitzel, *Dalton Trans.* **2017**, *46*, 1112–1123.
- [19] J. Tomaschautzky, B. Neumann, H.-G. Stammer, A. Mix, N. W. Mitzel, *Dalton Trans.* **2017**, *46*, 1645–1659.
- [20] A. Schwartz, M. Rovers, B. Neumann, H.-G. Stammer, N. W. Mitzel, *Eur. J. Org. Chem.* **2018**, 5323–5333.
- [21] a) E. Weisheim, C. G. Reuter, P. Heinrichs, Y. V. Vishnevskiy, A. Mix, B. Neumann, H.-G. Stammer, N. W. Mitzel, *Chem. Eur. J.* **2015**, *21*, 12436–12448; b) E. Weisheim, L. Buecker, B. Neumann, H.-G. Stammer, N. W. Mitzel, *Dalton Trans.* **2016**, *45*, 198–207; c) E. Weisheim, S. Weigel, B. Neumann, H.-G. Stammer, N. W. Mitzel, *Chem. Commun.* **2019**, *55*, 4985–4988.
- [22] H. H. Wenk, W. Sander, *Eur. J. Org. Chem.* **2002**, 3927–3935.
- [23] S. Takahashi, Y. Kuroyama, K. Sonogashira, N. Hagihara, *Synthesis* **1980**, 627–630.
- [24] G. Just, R. Singh, *Tetrahedron Lett.* **1987**, *28*, 5981–5984.
- [25] H. Irngartinger, L. Leiserowitz, G. M. J. Schmidt, *Chem. Ber.* **1970**, *103*, 1132–1156.
- [26] I. Hisaki, Y. Sakamoto, H. Shigemitsu, N. Tohnai, M. Miyata, S. Seki, S. Tagawa, *Chem. Eur. J.* **2008**, *14*, 4178–4187.
- [27] M. L. Bell, R. C. Chiechi, C. A. Johnson, D. B. Kimball, A. J. Matzger, W. B. Wan, T. J. R. Weakley, M. M. Haley, *Tetrahedron* **2001**, *57*, 3507–3520.
- [28] J. M. Kehoe, J. H. Kiley, J. J. English, C. A. Johnson, R. C. Petersen, M. M. Haley, *Org. Lett.* **2000**, *2*, 969–972.
- [29] A. Schwartz, *Dissertation: Organische Grundgerüste für dreizählige Lewis-Säuren*, Universität Bielefeld, **2018**.
- [30] K. Tahara, T. Fujita, M. Sonoda, M. Shiro, Y. Tobe, *J. Am. Chem. Soc.* **2008**, *130*, 14339–14345.
- [31] O. Š. Milijanić, K. P. C. Vollhardt, G. D. Whitener, *Synlett* **2003**, 29–34.
- [32] P. N. W. Baxter, A. A. Ouahabi, L. Karmazin, A. Varnek, J.-M. Strub, S. Cianferani, *Eur. J. Org. Chem.* **2019**, 6783–6795.
- [33] D. Solooki, J. D. Bradshaw, C. A. Tessier, W. J. Youngs, R. F. See, M. Churchill, J. D. Ferrara, *J. Organomet. Chem.* **1994**, *470*, 231–236.
- [34] a) M. Linnemannstöns, J. Schwabedissen, A. A. Schultz, B. Neumann, H.-G. Stammer, R. J. F. Berger, N. W. Mitzel, *Chem. Commun.* **2020**, *56*, 2252–2255; b) M. Linnemannstöns, J. Schwabedissen, B. Neumann, H.-G. Stammer, R. J. F. Berger, N. W. Mitzel, *Chem. Eur. J.* **2020**, *26*, 2169–2173; c) S. Blomeyer, M. Linnemannstöns, J. H. Nissen, J. Paulus, B. Neumann, H.-G. Stammer, N. W. Mitzel, *Angew. Chem. Int. Ed.* **2017**, *56*, 13259–13263; *Angew. Chem.* **2017**, *129*, 13443–13447.
- [35] D. Hellwinkel, *Die systematische Nomenklatur der Organischen Chemie. Eine Gebrauchsanweisung*, 5th ed., Springer, Berlin, **2006**, p. 27.
- [36] a) M. A. Beckett, D. S. Brassington, M. E. Light, M. B. Hursthouse, *J. Chem. Soc. Dalton Trans.* **2001**, 1768–1772; b) V. Gutmann, *Coord. Chem. Rev.* **1976**, *18*, 225–255; c) U. Mayer, V. Gutmann, W. Gerger, *Monatsh. Chem.* **1975**, *106*, 1235–1257.
- [37] M. A. Beckett, G. C. Strickland, J. R. Holland, K. S. Varma, *Polymer* **1996**, *37*, 4629–4631.
- [38] a) D. Hartmann, M. Schädler, L. Greb, *Chem. Sci.* **2019**, *10*, 7379–7388; b) A. Schwartz, L. Siebe, J. Schwabedissen, B. Neumann, H.-G. Stammer, N. W. Mitzel, *Eur. J. Org. Chem.* **2018**, 2533–2540.
- [39] I. B. Sivaev, V. I. Bregadze, *Coord. Chem. Rev.* **2014**, *270–271*, 75–88.
- [40] G. J. P. Britovsek, J. Ugoletti, A. J. P. White, *Organometallics* **2005**, *24*, 1685–1691.
- [41] E. L. Myers, C. P. Butts, V. K. Aggarwal, *Chem. Commun.* **2006**, 4434–4436.
- [42] A. Schnurr, M. Bolte, H.-W. Lerner, M. Wagner, *Eur. J. Inorg. Chem.* **2012**, 112–120.

Manuscript received: September 9, 2020

Revised manuscript received: October 14, 2020

Accepted manuscript online: October 15, 2020

Version of record online: December 23, 2020